Blucher Mechanical Engineering Proceedings
May 2014, vol. 1 , num. 1
www.proceedings.blucher.com.br/evento/10wccm

10th World Congress on Computational Mechanics
8-13 July 2012 • São Paulo • Brazil

TEMPERATURE GRADIENT DISCONTINUITY AWARE NUMERICAL SCHEME FOR SOLIDIFICATION PROBLEMS

Alejandro Cosimo, Víctor Fachinotti, Alberto Cardona

Centro Internacional de Métodos Computacionales en Ingeniería (CIMEC-INTEC), Universidad Nacional del Litoral-CONICET, Güemes 3450, S3000GLN Santa Fe, Argentina. Corresponding author: alecosimo@gmail.com

Abstract. *A new enriched finite element formulation for solving isothermal phase change problems is presented. The proposed method is a fixed domain one, where the discontinuity in the temperature gradient is represented by means of enriching the finite element space through a function whose definition admits a discontinuity in its derivative. Generally, in this kind of formulations, the location where to enrich (as the location of the solidification front), is determined through a level set auxiliary formulation. In this work a different approach is explored, this position is determined implicitly through a constraint that imposes that the temperature attained at the phase change boundary is the melting temperature. Some numerical examples to show the application of the method are presented and finally the conclusions are exposed.*

Keywords: *Enriched Finite Element Method, Solidification Problems, Stefan Problem, Phase Change Problems, XFEM*

1. INTRODUCTION

Solidification processes are of interest in many areas of engineering, such as welding mechanics [8], nuclear engineering [3] and metallurgy. When solidification of a pure substance is considered, the problem is described as an isothermal phase change problem characterized mainly by two parameters: the material melting temperature and its latent heat. One way to numerically solve this problem is through the use of a temperature based formulation with a fixed domain finite element technique in which remeshing is not needed [12].

An inherent difficulty of the considered problem is the discontinuity in the temperature gradient at the solidification front. From the point of view of stability and robustness, difficulties associated to this discontinuity appear with low sensible to latent heat ratios (Stefan number) or when the initial temperature is very closed to the melting temperature [20]. Classical Finite Element schemes cannot handle these situations efficiently, and require a large number of elements to get accurate solutions. In several scenarios, a standard Newton-Raphson solver does not converge and a line search must be used [18]. Nevertheless, in many situations the latter techniques are not enough to get convergence.

If attention is paid to fixed domain finite element techniques that perform discontinuous spatial integration, such as those proposed by Crivelli and Idelsohn [7] and subsequently refined by Storti *et al.* [23] and Fachinotti *et al.* [9], it is observed that in some situations oscillations in the converged solution exist. The reason is that for high latent heat values, the discontinuity in the temperature gradient is pronounced and it is not possible to represent such discontinuity when the position of the solidification front does not coincide with an element boundary. That is because the interpolated gradient inside the element is continuous. The situation gets worse if it is considered that most simulations are carried out with linear shape functions, so the representable gradients are piecewise constant. One way to avoid this situation is to introduce the representation of the gradient discontinuity inside elements. For this purpose an enriched finite element scheme is proposed.

Currently, the use of enriching techniques is quite spread in fluid and in fracture mechanics [10, 22, 2]. It should be noted that this is not the case for solidification problems. There are few enriched formulations in the literature for solving the previously mentioned types of phase change problems. Chessa *et al.* [5] and Bernauer and Herzog [4] determined the position of the enrichment through a level set function that is evolved with the interface Rankine-Hugoniot condition (specialised to the Stefan problem) and the associated advection equation. Several steps are performed to compute the solution of the level set equation [21]. First, the velocity of the solidification front is computed from the Stefan condition, and a velocity field is built by extending the velocity of the solidification front to the whole domain. Next, the level set equation is solved to move the interface. Finally, the standard heat equation is solved for each domain (solid and liquid) separately by imposing the interface constraint that dictates that the temperature at the phase change boundary must be equal to the melting temperature. The imposition of the mentioned constraint is enforced with a penalty formulation or a Lagrange multipliers formulation. Ji *et al.* [13] present a similar approach, differing from the previous one in the level set update and the energetically consistent way that they use to determine the jump in the heat flux at the interface. In contrast, Merle and Dolbow [17] proposed an enriched formulation in which they use an equation that is similar to a level set to track the interface position and the LATIN method [15] as iterative procedure to satisfy the local interface constraints stated by the problem.

The proposed numerical method is tested in one dimensional situations, for extreme values of temperature gradient discontinuity and characteristic temperatures. Comparisons with results obtained from a fixed mesh numerical scheme [9], where the temperature gradient discontinuity is not considered, are presented. Finally conclusions are presented.

2. MATHEMATICAL SETTING

Isothermal phase change problems are governed by the first principle of thermodynamics. Assuming the contribution of the mechanical energy to the total energy is negligible and considering the specific enthalpy $\mathcal{H}$ as thermodynamic potential, the temperature field T is computed by solving the heat balance equation

$$\rho\dot{\mathcal{H}} = Q + \nabla \cdot (k\nabla T) \qquad \forall\, (\boldsymbol{x}, t) \in \Omega_i \times (t_0, \infty) \tag{1}$$

where ρ is the density, k is the thermal conductivity, T is the temperature, Q is the external heat source per unit volume, and Ω_i for $i \in [s, l]$ are the solid and liquid domains. The temperature field should verify the initial conditions

$$T = T_0 \qquad \forall\, \boldsymbol{x} \in \Omega_i, t = t_0 \tag{2}$$

where $T_0(\boldsymbol{x})$ is the initial temperature field. Additionally, the following set of boundary conditions must be verified

$$T = T_d \qquad \forall\, (\boldsymbol{x}, t) \in \partial\Omega_d \times (t_0, \infty) \tag{3}$$

$$-(k\nabla T) \cdot \boldsymbol{n} = q_w \qquad \forall\, (\boldsymbol{x}, t) \in \partial\Omega_q \times (t_0, \infty) \tag{4}$$

$$-(k\nabla T) \cdot \boldsymbol{n} = h_f(T - T_f) \qquad \forall\, (\boldsymbol{x}, t) \in \partial\Omega_c \times (t_0, \infty) \tag{5}$$

where T_d is the imposed temperature at the boundary $\partial\Omega_d$, q_w is the external heat flow at the boundary $\partial\Omega_q$, h_f is the heat convection coefficient and T_f is the external fluid temperature at the portion the boundary $\partial\Omega_c$. Finally, at the interface Γ, which is determined by the phase change boundary, the constraint on the temperature and the Stefan condition hold

$$T = T_m \qquad \forall\, (\boldsymbol{x}, t) \in \Gamma \times (t_0, \infty) \tag{6}$$

$$[-(k\nabla T) \cdot \boldsymbol{n}]_\Gamma = \rho\mathcal{L}\boldsymbol{u}_\Gamma \qquad \forall\, (\boldsymbol{x}, t) \in \Gamma \times (t_0, \infty). \tag{7}$$

Here, $\mathcal{L}$ is the latent heat, T_m is the melting temperature, $\boldsymbol{u}_\Gamma$ is the velocity of the solidification front and the operator $[\centerdot]_\Gamma$ measures the jump of the quantity $\centerdot$ at the solidification front. Equation (6) is the constraint that imposes that the temperature at the phase change boundary must be equal to the melting temperature. Equation (7) is the interface condition (the Stefan condition).

2.1. Variational temperature based formulation

Let $\mathcal{S} = \{T/T \in \mathcal{H}^1(\Omega),\, w|_{\Gamma_d} = T_d\}$ be the space of trial solutions and $\mathcal{V} = \{v/v \in \mathcal{H}^1(\Omega),\, w|_{\Gamma_d} = 0\}$ be the space of weighting or test functions, where $\mathcal{H}^1$ is the first order Sobolev space.

It can be shown, following similar procedures presented in [7, 23, 9], that the strong form equations (1-7) can be made equivalent to the following weak temperature based formulation:

Find $T \in \mathcal{S}$ *such that* $\forall w \in \mathcal{V}$

$$\int_\Omega w \left[\rho c \frac{\partial T}{\partial t} + \rho\mathcal{L}\frac{\partial f_l}{\partial t} - Q\right] d\Omega + \int_\Omega \nabla w \cdot (k\nabla T)\, d\Omega + \int_{\Gamma_c} w h_f (T - T_f)\, d\Gamma_c + \int_{\Gamma_q} w q_w\, d\Gamma_q = 0 \tag{8}$$

3. ENRICHED FINITE ELEMENT FORMULATION

For solidification problems, there is a weak discontinuity, i.e. only the gradient of the temperature field is discontinuous at the solidification front. The main features of this discontinuity are its weakness and local behaviour. For the local behaviour, we only need to enrich

those elements that are crossed by the phase change boundary. For the weak discontinuity, the enrichment function only needs to have a discontinuity in its gradient.

A Galerkin finite element formulation is adopted for the discretisation of the continuous variational formulation. The enrichment functions are time dependent because of the change in position of the interface. Therefore, the space of weighting functions $\mathcal{V}$ depends on time, and the spatial and time discretisations need to be studied carefully. Following Fries and Zillian [11], the discretisation in time is first performed, and then the space discretisation is performed.

3.1. Enrichment Function Definition

The functional space of the element intersected by the interface (or solidification front) is enriched with a weak discontinuous function denoted by E. Two features need to be considered to build this function: E should have a local character and vanish at the element nodes, and ∇E must be discontinuous at the phase change boundary.

An enrichment function with these features was proposed by Coppola-Owen and Codina [6]. To isolate this concept, we restrict the analysis to the one dimensional case. To describe the position of the interface, we make use of a level set function ϕ defined by

$$\phi = x - x_a \tag{9}$$

where x_a is given by

$$x_a = x_1 + s(x_2 - x_1) = x_1 + sh \tag{10}$$

with x_1 the position of the left node, x_2 the position of the right node and h the element length. The interface is located at the point where the level set function ϕ equals zero. This position is provided locally by the parameter $s \in (0, 1)$, while its global position is tracked with x_a.

An example of the previously described enrichment function is provided in figure 1, and has a discontinuity at $s = 0.35$. For one dimensional cases, this enrichment is conforming but this is not true for higher dimensions.

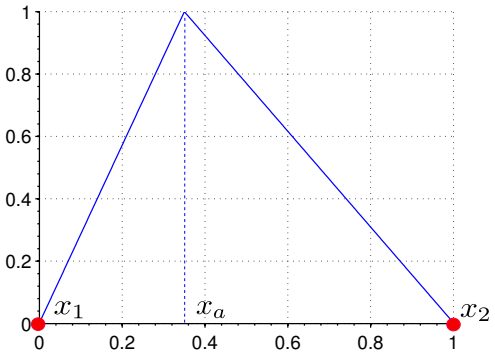

Figure 1. Enrichment function.

The definition of the enrichment function is given by

$$E(x) = \begin{cases} \dfrac{x - x_1}{x_a - x_1} = \dfrac{\phi_1 - \phi}{\phi_1} & x \leq x_a \\ \dfrac{x_2 - x}{x_2 - x_a} = \dfrac{\phi_2 - \phi}{\phi_2} & x > x_a \end{cases} \tag{11}$$

where $\phi_1 = x_1 - x_a$ and $\phi_2 = x_2 - x_a$. The temperature field inside an enriched element is described as

$$T(x,t) = \sum_i N_i(x) T_i + E(x,t) a \tag{12}$$

where the term $\sum N_i T_i$ corresponds to the usual finite element discretisation with N_i the shape functions and T_i the nodal degrees of freedom. The term $E(x,t)a$ corresponds to the enrichment, where $E(x,t)$ is the enrichment function and a is the associated degree of freedom. In the subsequent development linear shape functions are used.

3.2. Time Discretisation

By applying the divergence theorem to the weak formulation (8) over the entire domain Ω, we obtain the equation

$$\int_\Omega w \left[\rho c \frac{\partial T}{\partial t} + \rho \mathcal{L} \frac{\partial f_l}{\partial t} - \nabla \cdot (k \nabla T) - Q \right] d\Omega = 0 \qquad \forall w \in \mathcal{V} \tag{13}$$

An unconditionally stable backward Euler scheme is used to accomplish the temporal discretisation, obtaining the following result

$$\int_\Omega w \left[\rho c_{n+1} \frac{T_{n+1} - T_n}{\Delta t} + \rho \mathcal{L} \frac{f_{l(n+1)} - f_{l(n)}}{\Delta t} - \nabla \cdot (k_{n+1} \nabla T_{n+1}) - Q_{n+1} \right] d\Omega = 0 \tag{14}$$

where $c_{n+1} \equiv c(T_{n+1})$ and $k_{n+1} \equiv k(T_{n+1})$.

The time level for the evaluation of the test function w was not specified in equation (14). We choose w at the time level $n+1$, i.e. $w(x, t_{n+1}) \equiv w_{n+1}$, because if we choose to evaluate w at the time level n, the regularity of the system matrix cannot be guaranteed [11].

To elucidate this issue, consider the case where at time step n the phase change boundary is within element e, and at time step $n+1$ the phase change boundary must be within the neighboring element $e+1$. At time step n, element e is enriched whereas element $e+1$ is not. When the interface tries to evolve to element $e+1$, the weight function w_n is zero at that element, providing a null equation for the enrichment. Therefore, the system matrix would be singular.

3.3. Spatial Discretisation

Let $\mathcal{S}^h \subset \mathcal{S}$ and $\mathcal{V}^h \subset \mathcal{V}$ be N-dimensional subspaces of the trial and test functional spaces. The discrete variational formulation is given by

Given T_0^h, h_f, T_d^h *and* q_w, *find* $T^h = v^h + T_d^h$, *where* $v^h \in \mathcal{V}^h$ *and* $T^h|_{\Gamma_d} = T_d^h$, *such that*

$$\int_\Omega w_{n+1}^h \left[\rho c_{n+1} \frac{T_{n+1}^h - T_n^h}{\Delta t} + \rho \mathcal{L} \frac{f_{l(n+1)} - f_{l(n)}}{\Delta t} - \nabla \cdot (k_{n+1} \nabla T_{n+1}^h) - Q_{n+1}^h \right] d\Omega = 0 \tag{15}$$

$\forall w_{n+1}^h \in \mathcal{V}^h$.

For simplicity, it is assumed that $T_d^h = 0$, such that $T^h = v^h$. Applying the divergence theorem to equation (15), we obtain

$$\frac{1}{\Delta t}\int_\Omega \rho c_{n+1} w_{n+1}^h T_{n+1}^h \, d\Omega - \frac{1}{\Delta t}\int_\Omega \rho c_{n+1} w_{n+1}^h T_n^h \, d\Omega + \frac{1}{\Delta t}\int_\Omega \rho \mathcal{L} w_{n+1}^h f_{l(n+1)}^h \, d\Omega - \frac{1}{\Delta t}\int_\Omega \rho \mathcal{L} w_{n+1}^h f_{l(n)}^h \, d\Omega + \int_\Omega k_{n+1} \nabla T_{n+1}^h \cdot \nabla w_{n+1}^h \, d\Omega - \int_\Omega Q_{n+1}^h w_{n+1}^h \, d\Omega + \int_{\Gamma_q} w_{n+1}^h q_w \, d\Gamma_q + \int_{\Gamma_c} w_{n+1}^h h_{f_{n+1}} T_{n+1}^h \, d\Gamma_c + \int_{\Gamma_c} w_{n+1}^h h_{f_{n+1}} T_{f(n+1)} \, d\Gamma_c = 0 \quad (16)$$

The discrete test and trial functions $v^h \in \mathcal{V}^h$ are the set of usual linear finite element functions covering the whole domain, plus enrichment functions (11) at the elements that are crossed by the interface. Thus, a typical enriched finite element in the one dimensional case has a total of three shape functions (including the enrichment one). In matrix notation, $T^h \in \mathcal{V}^h$ inside an enriched element is given by

$$T^h = \boldsymbol{N}^T \boldsymbol{T} \quad (17)$$

where

$$\boldsymbol{N} = \begin{bmatrix} N_1(x) \\ N_2(x) \\ E(x,t) \end{bmatrix} \qquad \text{and} \qquad \boldsymbol{T} = \begin{bmatrix} T_1 \\ T_2 \\ a \end{bmatrix}. \quad (18)$$

The contribution of an enriched element to the residual, equation (16), is obtained

$$\boldsymbol{\Pi} = \frac{\boldsymbol{C}\boldsymbol{T}_{n+1}}{\Delta t} - \frac{\boldsymbol{C}^*\boldsymbol{T}_n}{\Delta t} + \frac{\boldsymbol{L}_{n+1} - \boldsymbol{L}_n}{\Delta t} + \boldsymbol{K}\boldsymbol{T}_{n+1} + \boldsymbol{F} - \boldsymbol{Q} \quad (19)$$

where

$$\boldsymbol{C} = \int_\Omega \rho c_{n+1} \boldsymbol{N}_{n+1} \boldsymbol{N}_{n+1}^T \, d\Omega \quad (20)$$

$$\boldsymbol{C}^* = \int_\Omega \rho c_{n+1} \boldsymbol{N}_{n+1} \boldsymbol{N}_n^T \, d\Omega \quad (21)$$

$$\boldsymbol{K} = \int_\Omega \nabla \boldsymbol{N}_{n+1} k_{n+1} \nabla \boldsymbol{N}_{n+1}^T \Omega + \int_{\Gamma_c} h_{f_{n+1}} \boldsymbol{N}_{n+1} \boldsymbol{N}_{n+1}^T \, d\Gamma_c \quad (22)$$

$$\boldsymbol{L}_{n+1} = \int_\Omega \rho \mathcal{L} \boldsymbol{N}_{n+1} f_{l(n+1)} \, d\Omega \quad (23)$$

$$\boldsymbol{L}_n = \int_\Omega \rho \mathcal{L} \boldsymbol{N}_{n+1} f_{l(n)} \, d\Omega \quad (24)$$

$$\boldsymbol{F} = \int_{\Gamma_q} \boldsymbol{N}_{n+1} q_{w_{n+1}} \, d\Gamma_q - \int_{\Gamma_c} h_{f_{n+1}} \boldsymbol{N}_{n+1} T_{f_{n+1}} \, d\Gamma_c \quad (25)$$

$$\boldsymbol{Q} = \int_\Omega \boldsymbol{N}_{n+1} Q_{n+1} \, d\Omega \quad (26)$$

It is worthwhile to mention that function $\boldsymbol{N}_{n+1}$ depends on the interface position, which is an unknown of the problem, incrementing the degree of non linearity of the equations. The nonlinear problem (19) is solved using a Newton-Raphson scheme

$$\boldsymbol{\Pi}^{(i+1)} \simeq \boldsymbol{\Pi}^{(i)} + \frac{\partial \boldsymbol{\Pi}}{\partial \boldsymbol{T}}^{(i)} (\boldsymbol{T}^{(i+1)} - \boldsymbol{T}^{(i)}) = \boldsymbol{0} \quad (27)$$

where i represents the i^{th} iteration. Note that we eliminated the subscript $n+1$ to simplify notation.

Iterations proceed until convergence (the norm of the residual meets a prescribed tolerance). Due to the high non linearity of the problem, a line-search method must be used in conjunction with the Newton-Raphson scheme. This type of globally convergent method is quite standard and its formulation can be found in most textbooks that consider nonlinear optimisation problems [25, 14].

3.4. Determination of the interface position

The determination of the interface position is essential for this method because the enriched shape functions depend on it. As previously mentioned, in other enrichment formulations, the interface position is computed using an auxiliary level set equation. After this position is determined, the standard heat conduction equation is solved in each subdomain, enriching the elements that are intersected by the phase change boundary. Additionally, the constraint (6) is imposed through the use of Lagrange multipliers or a penalty formulation.

We are proposing a new way to determine the interface position implicitly at each Newton iteration in terms of the values of the degrees of freedom corresponding to that iteration and the constraint given by equation (6). Suppose that we are processing iteration i and we have the guess values $\boldsymbol{T}^{(i)}$. With these guess values, we determine if the element that is being processed is intersected by the solidification front. If this is the case, the value of the parameter s is calculated by applying the constraint given by equation (6).

When using the enrichment functions defined in equation (11), a closed form of the value of the parameter s can be determined, which is given by

$$s = \frac{T_m - T_1^{(i)} - a^{(i)}}{T_2^{(i)} - T_1^{(i)}} \tag{28}$$

This procedure is based on physical features more than other methods due to determination of the interface position with the current temperature distribution.

3.5. Discontinuous integration

When processing an enriched element, a weak discontinuity appears in the element, which requires discontinuous integration of the terms from equations (20) to (26). The number of integration regions depends on the nature of the integrand, i.e. the integrand only depends on the time step at $n+1$ or it depends on both time steps n and $n+1$. In the former case, we have two subregions, in the latter case we typically have three subregions.

The integration is performed numerically using a Gaussian quadrature. Selection of the integration rule depends on the number of subregions. For instance, suppose that we are processing an enriched element, and we are calculating the term described by equation (21) with three subregions. Then, the integration rule is given by

$$\boldsymbol{C}^* = \int_\Omega \rho c \boldsymbol{N}_{n+1} \boldsymbol{N}_n^T \, d\Omega = \sum_{p=1}^{3} \sum_{g=1}^{n_g} \rho c \boldsymbol{N}_{n+1}(x_g^{(p)}) \boldsymbol{N}_n^T(x_g^{(p)}) w_g \Omega^{(p)} \tag{29}$$

where the index p of the outer sum indicates the partition or region number (ranging in this case from one to three), the index g of the inner sum indicates the Gaussian point being evaluated, n_g is the number of Gaussian points and w_g are the Gaussian weights [19].

3.6. Tangent matrix

After differentiating the nonlinear residual function (19) with respect to the generalised degrees of freedom $\boldsymbol{T}$, we obtain

$$\frac{\partial \boldsymbol{\Pi}}{\partial \boldsymbol{T}} = \frac{\boldsymbol{C}}{\Delta t} + \boldsymbol{K} + \frac{1}{\Delta t}\frac{\partial \boldsymbol{C}}{\partial \boldsymbol{T}}\boldsymbol{T}^{(i)} - \frac{1}{\Delta t}\frac{\partial \boldsymbol{C}^*}{\partial \boldsymbol{T}}\boldsymbol{T}_n + \frac{\partial \boldsymbol{K}}{\partial \boldsymbol{T}}\boldsymbol{T}^{(i)} + \frac{1}{\Delta t}\frac{\partial \boldsymbol{L}_{n+1}}{\partial \boldsymbol{T}} - \frac{1}{\Delta t}\frac{\partial \boldsymbol{L}_n}{\partial \boldsymbol{T}} + \frac{\partial \boldsymbol{F}}{\partial \boldsymbol{T}} - \frac{\partial \boldsymbol{Q}}{\partial \boldsymbol{T}} \quad (30)$$

The first two terms on the right-hand-side are standard in any nonlinear thermal problem. The other terms have certain particularities in the enriched elements, which will be described. We first consider the case in which thermophysical properties do not depend on temperature. Contributions to the tangent matrix arising from temperature dependent thermophysical properties will be later considered.

As previously described, the computation of the mentioned terms in an enriched element depends on the number of subregions. We study the case with the term $\frac{\partial \boldsymbol{C}^*}{\partial \boldsymbol{T}}$; the other terms in equation (30) are computed similarly.

There are three sources where $\boldsymbol{C}^*$ depends on $\boldsymbol{T}$:

- *Evaluation dependency*: the integration region depends on the position of the discontinuity at the time step $n+1$. Therefore, the position of the Gauss points in the physical space depends implicitly on the degrees of freedom $\boldsymbol{T}$.
- *Enrichment dependency*: the position for the enrichment is always determined in terms of the degrees of freedom $\boldsymbol{T}$, so the enrichment function definition depends on $\boldsymbol{T}$.
- *Integration region dependency*: when discontinuous integration is applied and the integration region is determined by the position of the interface at time step $n+1$. An implicit dependency on the degrees of freedom $\boldsymbol{T}$ is present.

Considering the outlined dependencies, the derivative $\frac{\partial \boldsymbol{C}^*}{\partial \boldsymbol{T}}$ is given by

$$\frac{\partial C^*_{rk}}{\partial T_j} = \sum_{p=1}^{3}\sum_{g=1}^{n_g} \rho c \left[\frac{\partial N_{n+1(r)}}{\partial x_g^{(p)}}\frac{\partial x_g^{(p)}}{\partial s}\frac{\partial s}{\partial T_j} N_{n(k)} w_g \Omega^{(p)} + N_{n+1(r)}\frac{\partial N_{n(k)}}{\partial x_g^{(p)}}\frac{\partial x_g^{(p)}}{\partial s}\frac{\partial s}{\partial T_j} w_g \Omega^{(p)} + \frac{\partial N_{n+1(r)}}{\partial x_a}\frac{\partial x_a}{\partial s}\frac{\partial s}{\partial T_j} N_{n(k)} w_g \Omega^{(p)} + N_{n+1(r)} N_{n(k)} w_g \frac{\partial \Omega^{(p)}}{\partial s}\frac{\partial s}{\partial T_j} \right] \quad (31)$$

The definition of x_a is given by equation (10). The first two terms in equation (31) arise from the *evaluation dependency*, the third term arises from the *enrichment dependency* and the fourth term arises from the *integration region dependency*. Computation of the terms $\frac{\partial x_g^{(p)}}{\partial s}$,

$\frac{\partial x_a}{\partial s}$ and $\frac{\partial \Omega^{(p)}}{\partial s}$ are straightforward

$$\begin{array}{lll} \dfrac{\partial x_g^{(1)}}{\partial s} = 0 & & \dfrac{\partial \Omega^{(1)}}{\partial s} = 0 \\ \dfrac{\partial x_g^{(2)}}{\partial s} = \xi_2 h & \dfrac{\partial x_a}{\partial s} = h & \dfrac{\partial \Omega^{(2)}}{\partial s} = h \\ \dfrac{\partial x_g^{(3)}}{\partial s} = (1-\xi_3) h & & \dfrac{\partial \Omega^{(3)}}{\partial s} = -h \end{array} \tag{32}$$

where $\xi_i, i = 1, 2, 3$ are the natural coordinates for each integration region.

The computation of the derivative $\frac{\partial s}{\partial T_j}$ is more cumbersome. By linearising the increment of $T(\boldsymbol{T}, x, s)$ and working the first order terms, it can be shown that $\frac{\partial s}{\partial \boldsymbol{T}}$ is given by

$$\frac{\partial s}{\partial \boldsymbol{T}} = \left(\sum_{i=1}^{2} h \frac{\partial N_i}{\partial x}(x_a)\, T_i \right)^{-1} \begin{bmatrix} N_1(x_a) \\ N_2(x_a) \\ 1 \end{bmatrix} \tag{33}$$

4. NUMERICAL EXAMPLES

The proposed method was tested for difficult problems, i.e., problems with extreme values of temperature gradient discontinuity and with initial temperatures close to the melting temperature. The obtained results were compared with analytic solutions and with the results obtained from the fixed mesh numerical scheme presented in [9], where the temperature gradient discontinuity was not considered.

4.1. Problem I, the Two Phase Stefan Problem: Dirichlet boundary conditions

Here, we study the freezing of a long slab that was initially at temperature T_0 above the melting temperature T_m and is suddenly cooled by imposing a constant temperature $T_1 < T_m$ to the slab end $x = 0$. The temperature at the slab end $x = L$ is held at $T_0 > Tm$, where L is the slab length. Similar simulations were presented in references [16, 17]. The parameters of the problem are given in table 1.

Table 1. Problem I parameters

$\mathcal{L}$	c_s	c_l	k_s	k_l
$190.26 \frac{\mathrm{J}}{\mathrm{kg}}$	$0.49 \frac{\mathrm{J}}{^\circ\mathrm{Ckg}}$	$0.62 \frac{\mathrm{J}}{^\circ\mathrm{Ckg}}$	$9.6 \times 10^{-3} \frac{W}{^\circ\mathrm{Cm}}$	$6.9 \times 10^{-3} \frac{W}{^\circ\mathrm{Cm}}$
ρ	T_m	T_1	L	T_0
$1 \frac{\mathrm{kg}}{\mathrm{m}^3}$	$0\,^\circ\mathrm{C}$	$-10\,^\circ\mathrm{C}$	$10\mathrm{m}$	$4\,^\circ\mathrm{C}$

Sixteen equally spaced elements and a time step of $18\mathrm{s}$ are used to model this problem. The computed solution is shown in figure 2 for different time instants and is compared with the analytic solution for a semi-infinite medium [24] showing almost perfect agreement. Additionally, the solution obtained with the formulation without enrichment proposed by Fachinotti

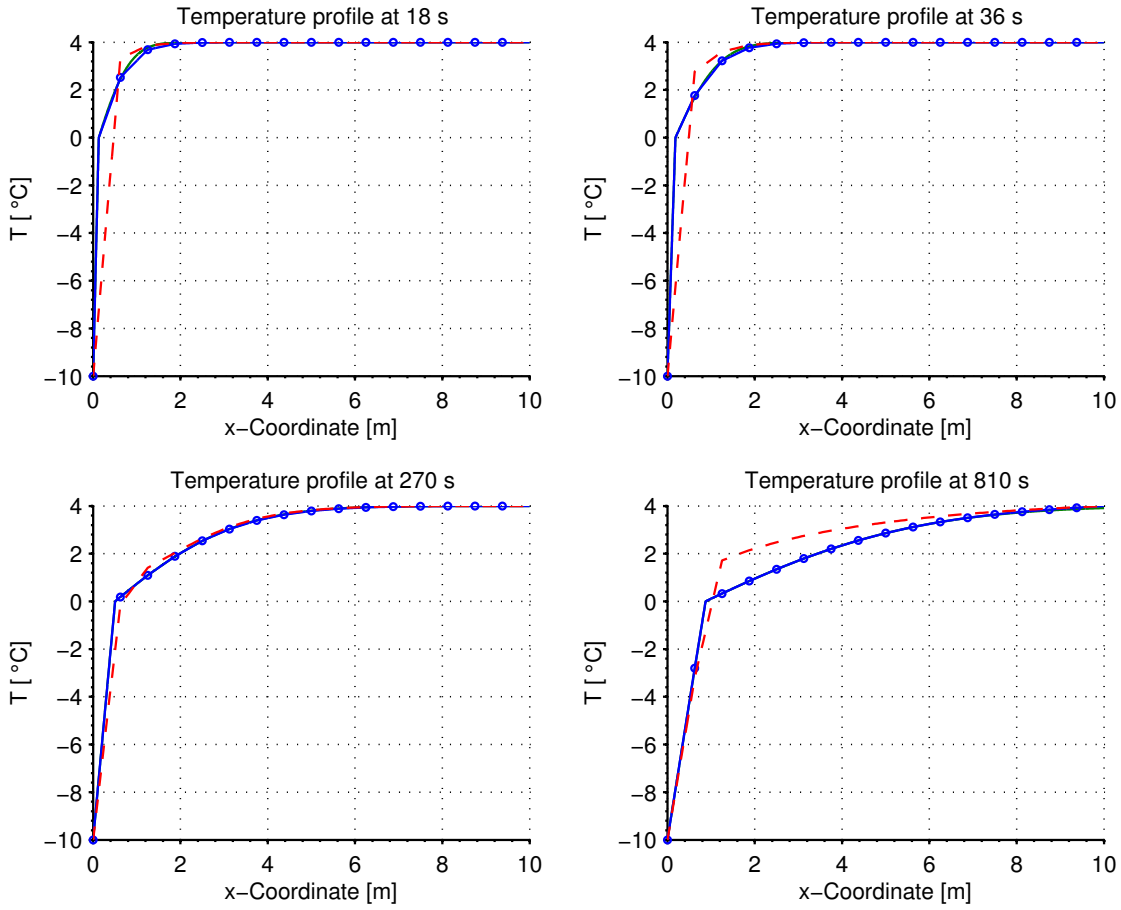

Figure 2. Solution of problem I at different time steps. The solid line is the exact solution. The dashed line is the approximate solution without enrichment. The solid line with circles is the approximate solution obtained with the proposed method.

et al. [9] is shown in dashed lines. The solution without enrichment presents spurious oscillations and, in certain time instants, is quite different from the analytic solution.

Figure 3 displays the interface evolution over time. Again, the current method shows almost perfect agreement with the analytical solution, while the formulation without enrichment differs from the analytic solution. Figure 4 provides the temperature evolution at node 2 ($x = 0.625$ m); the previous comments apply to this case as well.

Figure 5 presents the results when the mesh is refined using 32 equally spaced elements. The temperature evolution at node 3 ($x = 0.625$ m) is shown. The result obtained with the proposed method is accurate while the result obtained with the method without enrichment is not. In addition, for the method without enrichment, the spurious oscillations increased their amplitude with respect to the mesh with 16 elements.

The quadratic convergence rate was observed in all time steps. The mean number of iterations per time step was 3.62, and the maximum number of iterations at a given time step was 12. These values are similar to those for the fixed mesh technique, which required 3.32 iterations per time step, with a maximum of 7 iterations.

In table 2 the evolution of the residual for a number of representative time steps can be observed. The maximum number of iterations is attained at the first time step ($t = 18$

Table 2. Iterations from the proposed formulation for select time steps.

Iteration	Time 18s	Time 126s	Time 234s	Time 324s
1	8.7324	0.3203	0.2482	0.2227
2	7.1675	0.0109	0.0053	0.0037
3	5.8934	0.0001	2.5e-5	8.6e-6
4	4.8354	1.1e-9	2e-10	5.5e-11
⋮	⋮			
10	0.0654			
11	0.0025			
12	4.6e-6			

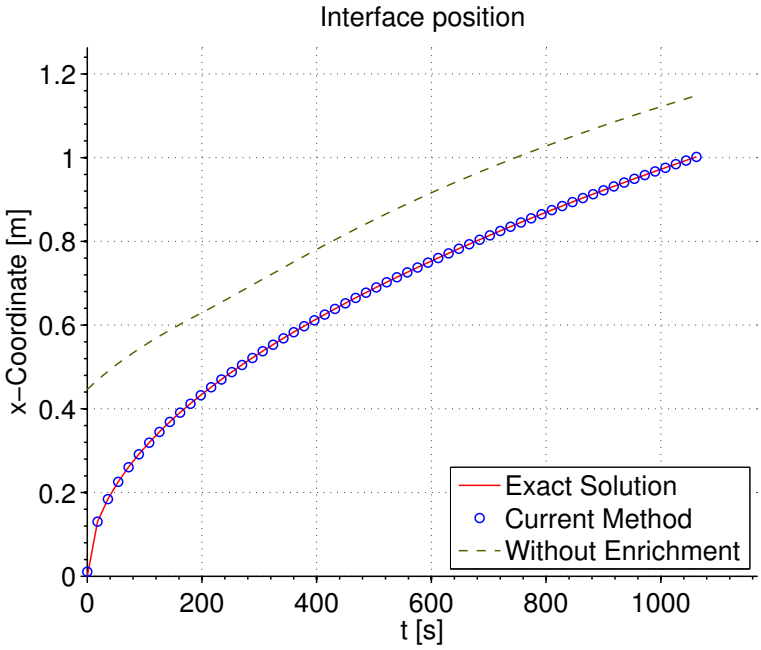

Figure 3. Interface position with exact and approximate values.

s) because at the initial time ($t = 0$ s), the interface is located too close to the first node to accurately represent the initial condition (a Heaviside at $x = 0$). It should be noted that the element's capability to represent this type of temperature distribution causes the observed accurate results. If the initial position of the interface is placed farther from $x = 0$, the number of iterations will be smaller, but the approximation to the exact solution of the problem will be less accurate. The errors with the method without enrichment are due, in part, to the impossibility of this formulation of representing this initial condition.

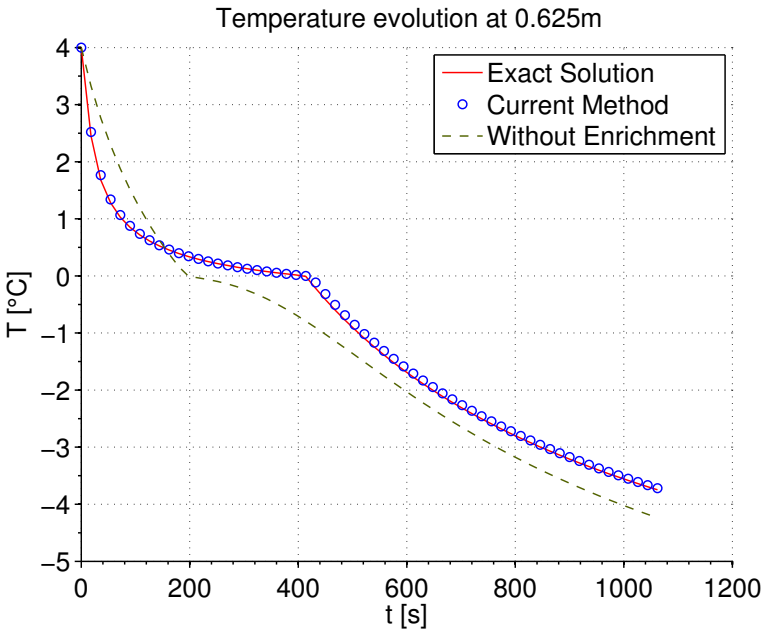

Figure 4. Temperature evolution with exact and approximate values. Spatial discretisation with 16 equally spaced elements.

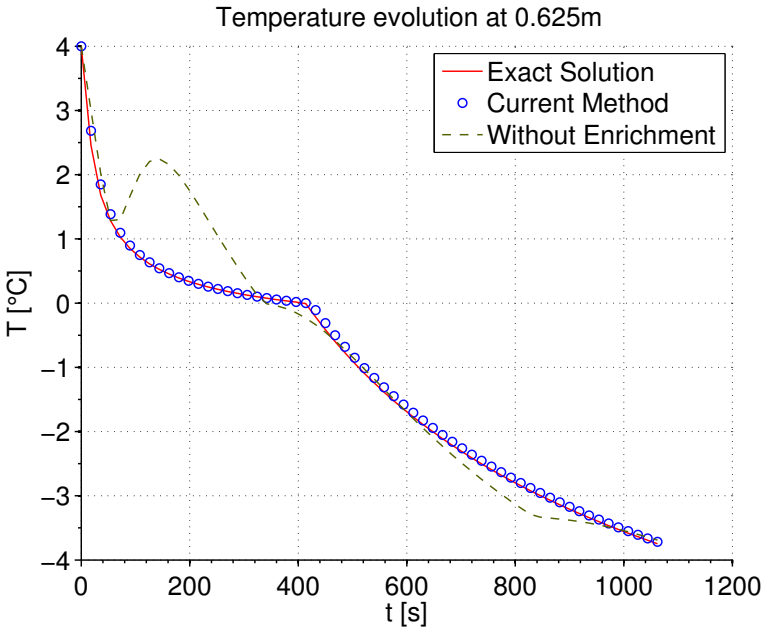

Figure 5. Temperature evolution with exact and approximate values. Spatial discretisation with 32 equally spaced elements.

4.2. Problem II, the Two Phase Stefan Problem: Dirichlet / Neumann boundary conditions

Here, we study the melting of a long slab initially at temperature T_0 below the melting temperature T_m that is suddenly heated by imposing a constant temperature $T_1 > T_m$ at the slab end $x = 0$. The slab end $x = L$ is insulated, where L is the slab length. The analytic solution for a semi-infinite medium associated with this problem can be found in [1].

The thermophysical parameters are considered constant and equal in both phases, such that $c = c_s = c_l$ and $k = k_s = k_l$. The problem parameters are given in table 3.

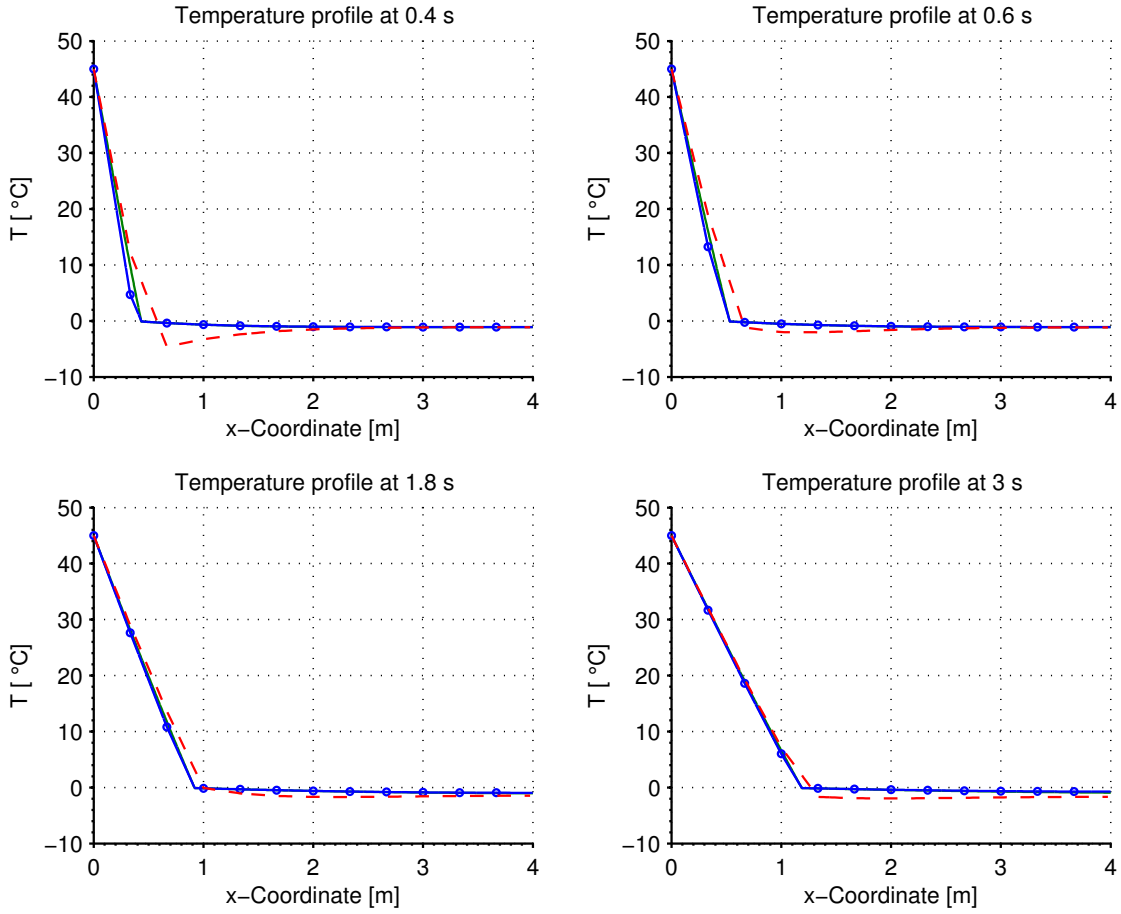

Figure 6. Solution of problem II at different time steps. The solid line is the exact solution. The dashed line is the approximate solution without enrichment. The solid line with circles is the approximate solution obtained with the proposed method.

Twelve equally spaced elements and a time step of 0.2s are used to model this problem. The computed solution is shown in figure 6 for different time instants and is compared with the analytic solution, showing almost perfect agreement. Additionally, the solution obtained using the formulation without enrichment, proposed by Fachinotti *et al.* [9], is shown with dashed lines. The solution without enrichment includes spurious oscillations, and in certain time instants is quite different from the analytic solution.

Figure 7 displays the interface evolution over time. Again, the method with enrichment shows nearly perfect agreement with the analytical solution, while the formulation without enrichment does not. In figure 8 the temperature evolution at node 2 ($x = 0.33$ m) is provided.

Table 3. Parameters of problem II

$\mathcal{L}$	c	k	ρ
$190.26\frac{\mathrm{J}}{\mathrm{kg}}$	$1\frac{\mathrm{J}}{^{\circ}\mathrm{Ckg}}$	$1.08\frac{W}{^{\circ}\mathrm{Cm}}$	$1\frac{\mathrm{kg}}{\mathrm{m}^3}$
T_m	T_1	L	T_0
$-0.1\,^{\circ}\mathrm{C}$	$45\,^{\circ}\mathrm{C}$	$4\mathrm{m}$	$-1.1\,^{\circ}\mathrm{C}$

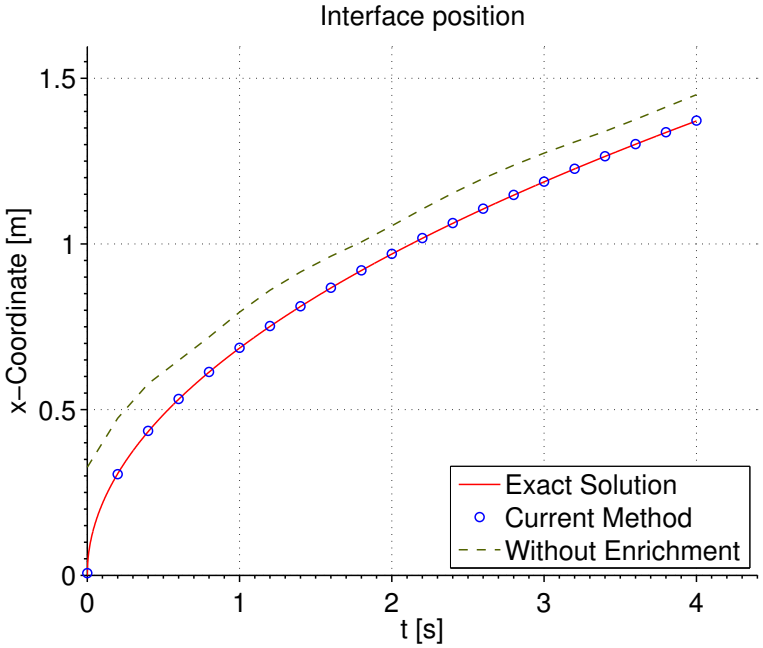

Figure 7. Interface position with exact and approximate values.

The enriched solution follows the analytic solution quite well, while the solution without enrichment has severe oscillations.

The Stefan number St_l for this problem is given by

$$\mathrm{St}_l = \frac{c_l(T_l - T_m)}{\mathcal{L}} = 0.23704 \tag{34}$$

The computational effort in this problem was important because of the high nonlinearity from our formulation. The mean number of iterations per time step was 17.89, and the maximum number of iterations at a given time step was 65. These values are much greater than those acquired with the fixed mesh technique, which required 5.25 iterations per time step with a maximum of 9 iterations. Nevertheless, the computed solution showed high accuracy, such that even though the Stefan number was small, the solution was quite close to the analytical solution and did not have spurious oscillations (these oscillations are undesirable, e.g., when computing the microstructure, which depends on the temperature history and on the temperature rates).

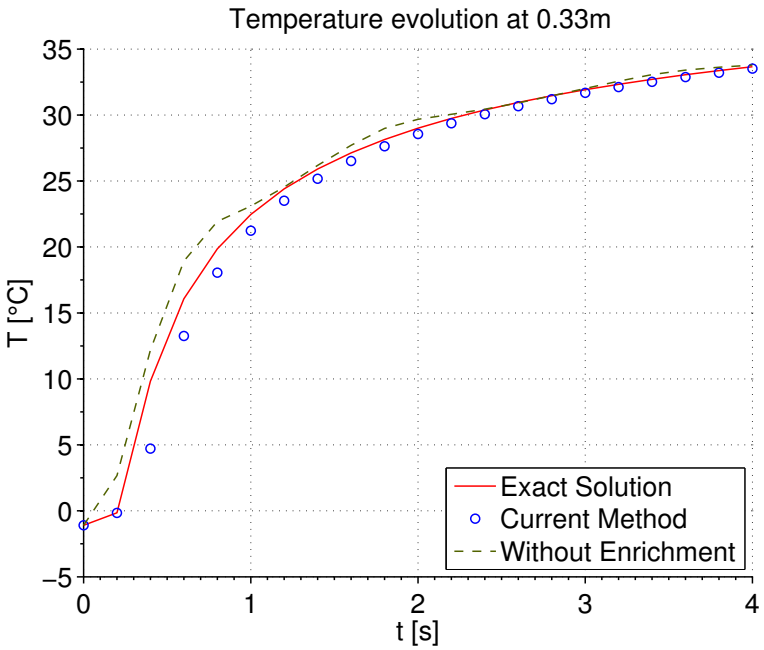

Figure 8. Temperature evolution with exact and approximate values.

5. CONCLUSIONS

A different approach for solving isothermal phase change problems is presented. The method has the advantages of a fixed mesh method as it does not need remeshing to conform to the phase change interface, but at the same time it introduces the possibility to represent the discontinuity in the temperature gradient at the solidification front by enriching locally where it is necessary. The position where to enrich is not determined through an auxiliary level set formulation as usual, instead this position is determined iteratively by means of the constraint that impose that the temperature at the phase change boundary must be the melting temperature.

Different test problems were investigated. The proposed method ran these tests giving results that were more accurate than with a formulation without enrichment and without presenting any spurious oscillations. In future work, the formulation of two and three-dimensional problems with temperature dependent thermophysical properties will be considered.

Acknowledgements

This work has received financial support from Consejo Nacional de Investigaciones Científicas y Técnicas (CONICET), Universidad Nacional del Litoral (UNL) and Autoridad Regulatoria Nuclear (ARN).

6. REFERENCES

[1] V. Alexiades and A. D. Solomon. *Mathematical Modeling of Melting and Freezing Processes.* Hemisphere Publishing Corporation, Taylor and Francis Group, 1993.

[2] R. F. Ausas, G. C. Buscaglia, and S. R. Idelsohn. A new enrichment space for the treatment of discontinuous pressures in multi-fluid flows. *International Journal for Numerical Methods in Fluids*, 2011. ISSN 1097-0363.

[3] F. Basombrío. El problema de dos fases en materiales heterogéneos. aplicaciones. *Revista internacional de métodos numéricos*, 13(3):351–366, 1997.

[4] M. Bernauer and R. Herzog. Implementation of an X-FEM solver for the classical two-phase Stefan problem. *Journal of Scientific Computing*, pages 1–23, 2011. ISSN 0885-7474.

[5] J. Chessa, P. Smolinski, and T. Belytschko. The extended finite element method (XFEM) for solidification problems. *International Journal for Numerical Methods in Engineering*, 53(8):1959, 2002.

[6] A. H. Coppola-Owen and R. Codina. Improving eulerian two-phase flow finite element approximation with discontinuous gradient pressure shape functions. *International Journal for Numerical Methods in Fluids*, 49(12):1287–1304, 2005. ISSN 1097-0363.

[7] L. A. Crivelli and S. R. Idelsohn. A temperature-based finite element solution for phase-change problems. *International Journal for Numerical Methods in Engineering*, 23(1): 99–119, 1986. ISSN 1097-0207.

[8] V. Fachinotti, A. Cardona, A. Cosimo, B. Baufeld, and O. Van der Biest. Evolution of temperature during shaped metal deposition: Finite element predictions vs. observations. *Mecánica Computacional*, 19:4915–4926, 2010.

[9] V. D. Fachinotti, A. Cardona, and A. E. Huespe. A fast convergent and accurate temperature model for phase-change heat conduction. *International Journal for Numerical Methods in Engineering*, 44(12):1863–1884, 1999. ISSN 1097-0207.

[10] T.-P. Fries and T. Belytschko. The extended/generalized finite element method: An overview of the method and its applications. *International Journal for Numerical Methods in Engineering*, 2010.

[11] T.-P. Fries and A. Zilian. On time integration in the XFEM. *International Journal for Numerical Methods in Engineering*, 79(1):69, 2009.

[12] S. Idelsohn, M. Storti, and L. Crivelli. Numerical methods in phase-change problems. *Archives of Computational Methods in Engineering*, 1:49–74, 1994.

[13] H. Ji, D. Chopp, and J. E. Dolbow. A hybrid extended finite element/level set method for modeling phase transformations. *International Journal for Numerical Methods in Engineering*, 54(8):1209–1233, 2002. ISSN 1097-0207.

[14] C. T. Kelley. *Iterative Methods for Optimization.* Society for Industrial and Applied Mathematics, Philadelphia, 1999.

[15] P. Ladevéze and J. G. Simmonds. *Nonlinear computational structural mechanics: new approaches and non-incremental methods of calculation.* Springer, 1999.

[16] D. R. Lynch and K. O'Neill. Continuously deforming finite elements for the solution of parabolic problems, with and without phase change. *International Journal for Numerical Methods in Engineering*, 17(1):81–96, 1981. ISSN 1097-0207.

[17] R. Merle and J. Dolbow. Solving thermal and phase change problems with the extended finite element method. *Computational Mechanics*, 28(5):339, 2002.

[18] A. K. Nallathambi, E. Specht, and A. Bertram. Computational aspects of temperature-based finite element technique for the phase-change heat conduction problem. *Computational Materials Science*, 47(2):332, 2009.

[19] N. Nigro, A. Huespe, and V. Fachinotti. Phasewise numerical integration of finite element method applied to solidification processes. *International Journal of Heat and Mass Transfer*, 43(7):1053–1066, 2000.

[20] M. Salcudean and Z. Abdullah. On the numerical modelling of heat transfer during solidification processes. *International Journal for Numerical Methods in Engineering*, 25(2):445–473, 1988. ISSN 1097-0207.

[21] J. A. Sethian. *Level Set Methods and Fast Marching Methods.* Cambridge University Press., 1996.

[22] A. Simone. Partition of unity-based discontinuous finite elements: GFEM, PUFEM, XFEM. *Revue européenne de génie civil*, 11(7-8):1045, 2007.

[23] M. Storti, L. A. Crivelli, and S. R. Idelsohn. Making curved interfaces straight in phase-change problems. *International Journal for Numerical Methods in Engineering*, 24(2): 375–392, 1987. ISSN 1097-0207.

[24] D. A. Tarzia. *Advanced Topics in Mass Transfer*, chapter 20, pages 439–484. InTech, 2011.

[25] P. Wriggers. *Nonlinear Finite Element Methods.* Springer, Berlin, 2008.